

## Growth of stoichiometric subnanometer silica films

D. J. Stacchiola,<sup>a)</sup> M. Baron, S. Kaya, J. Weissenrieder,  
S. Shaikhutdinov, and H.-J. Freund

*Fritz-Haber-Institut der Max-Planck-Gesellschaft, Faradayweg 4-6, 14195 Berlin, Germany*

(Received 4 July 2007; accepted 24 November 2007; published online 4 January 2008)

We present a method to grow stoichiometric SiO<sub>2</sub> films of only ~0.6–0.9 nm in thickness on a metal substrate. Based on photoelectron and infrared spectroscopy studies, we conclude that the ~0.6-nm-thick silica films exhibit characteristics only observed for >2.0-nm-thick films grown on conventional Si substrates. The films can be used as model oxides for fundamental studies and may have implications on the further miniaturization of metal-oxide-semiconductor transistors.

© 2008 American Institute of Physics. [DOI: 10.1063/1.2824842]

Thin oxide films are widely used for technical applications in electronics, sensors, and catalysis.<sup>1</sup> Current metal-oxide-semiconductor (MOS) transistors use SiO<sub>2</sub> films of ~1.3 nm in thickness as the gate dielectric. However, further miniaturization is in part inhibited by the presence of a ~0.6 nm transition region of substoichiometric SiO<sub>x</sub> at the SiO<sub>2</sub>/Si interface,<sup>2</sup> which prevents the formation of high-quality films of thickness <1.0 nm. Improvements in the quality of ultrathin films can be achieved through fine tuning the interface properties and/or the conditions for film growth.

It has been reported that SiO<sub>2</sub> films can be grown on Mo substrates, with thicknesses ranging from thick amorphous<sup>3</sup> to ultrathin crystalline “monolayer”<sup>4</sup> films. In the latter case, the metal substrate can influence particles deposited on the oxide film,<sup>5</sup> e.g., Pd and V deposited on monolayer SiO<sub>2</sub> penetrate through the film.<sup>6</sup> The use of different oxidants can further influence the stoichiometry and morphology of the oxide films. Metal deposition on water/ice layers can produce three-dimensional oxide particles<sup>7</sup> or films,<sup>8</sup> while deposition in oxygen generally leads to the formation of homogenous films.<sup>1</sup> The initial step in the oxidation of Si by water has been studied,<sup>9</sup> but further knowledge on the influence of water during the growth of oxide films is required.

Monolayer SiO<sub>2</sub> films grown on Mo(112) consist of a two-dimensional network of corner-sharing (SiO<sub>4</sub>) tetrahedra with one oxygen pointing towards the substrate (model in Fig. 1).<sup>10,11</sup> Attempts to grow additional layers on top of the monolayer film result in the formation of ill-defined structures. The lack of layer-by-layer growth can be explained by the saturated oxygen termination of the monolayer film and the strong interfacial Mo–O–Si bonds. Thus, in order to grow high quality multilayer films we reversed the interface, growing the SiO<sub>2</sub> from interfacial Mo–Si–O linkages. We report here on the synthesis of SiO<sub>2</sub> films with thickness in the subnanometer range characterized by low energy electron diffraction (LEED), x-ray photoelectron spectroscopy (XPS), infrared reflection absorption spectroscopy (IRAS), and scanning tunneling microscopy (STM). Pd was deposited on the films to study the stability of the system against diffusion and to reveal changes in the surface morphology of the oxides when using either water or oxygen as oxidant during film growth.

The experiments were carried out in an ultrahigh vacuum (UHV) chamber.<sup>4</sup> IR spectra were measured with *p*-polarized light at 84° grazing angle of incidence. The binding energies (BE) in XP spectra were calibrated relative to the Fermi edge of the Mo crystal. Si was evaporated from a rod. Three methods were used to grow multilayer SiO<sub>2</sub> films on Mo(112). Method 1: deposition in UHV of ≥3 MLE (“monolayer equivalents,” defined here as the amount of Si in a monolayer SiO<sub>2</sub>/Mo(112) film<sup>10</sup>) of Si at 300 K and oxidation at 400 K in 5 × 10<sup>-7</sup> mbar of O<sub>2</sub>. Method 2: deposition of ~1 MLE of Si at 300 K, annealing at 1200 K, exposure at 350 K to 500 L of H<sub>2</sub>O (1 L = 1 × 10<sup>-6</sup> Torr s), and cycles of Si deposition and exposure to H<sub>2</sub>O at 350 K. Method 3: deposition of 2 MLE Si at 300 K, growth of a water/ice layer, and cycles of Si deposition and growth of ice layers at 100 K. In all methods, the films were annealed at 900 K in 5 × 10<sup>-7</sup> mbar of O<sub>2</sub> and then flashed to 1150 K under UHV. Only results for 2 and 3 MLE films are presented, but the methods also work for thicker films.

After deposition of Si at 300 K on the Mo(112) substrate and annealing to 1200 K, a surface alloy with a *p*(2 × 1) LEED pattern is formed. XPS studies (Fig. 1) show that the BE of the Si 2*p* level shifts from the bulk Si<sup>0</sup> state (at 99.5 eV) to 99.1 eV after annealing, in agreement with a previous study on the formation of a Mo silicide on Si/Mo(100).<sup>12</sup> This modified Si/Mo(112) interface, produced in all methods presented here, was used as the substrate to growth SiO<sub>2</sub> films. The thickness of the films was determined from the XPS integral intensity of Si<sup>4+</sup>, derived from the deconvolution of the Si 2*p* spectrum using a Shirley background and five chemical states.<sup>2</sup> The O 1*s* region of the monolayer film shows two components that have been assigned to oxygen in Mo–O–Si (531.2 eV) and Si–O–Si (532.5 eV) bonds.<sup>11</sup> For multilayer films, only one peak corresponding to oxygen in a SiO<sub>2</sub> environment<sup>3</sup> is observed at 533.1 eV, hence, proving the absence of Mo–O– bonds in films prepared with the current recipes. Since the films are inert toward CO adsorption as found by IRAS, the presence of metallic or partially oxidized Si on the surface can be ruled out, and the peak at 99.5 eV in the Si 2*p* region of the 2 MLE film is therefore assigned to Si<sup>0</sup> at the interface. At least ~0.6 MLE of Si<sup>0</sup> was required at the interface to prevent formation of Mo–O– bonds. A schematic model of the multilayer SiO<sub>2</sub>/Mo interface is included in Fig. 1. The absence of Si<sup>+3</sup> species in the Si 2*p* spectrum is consistent with

<sup>a)</sup> Author to whom correspondence should be addressed. Electronic mail: dstacchi@fhi-berlin.mpg.de.

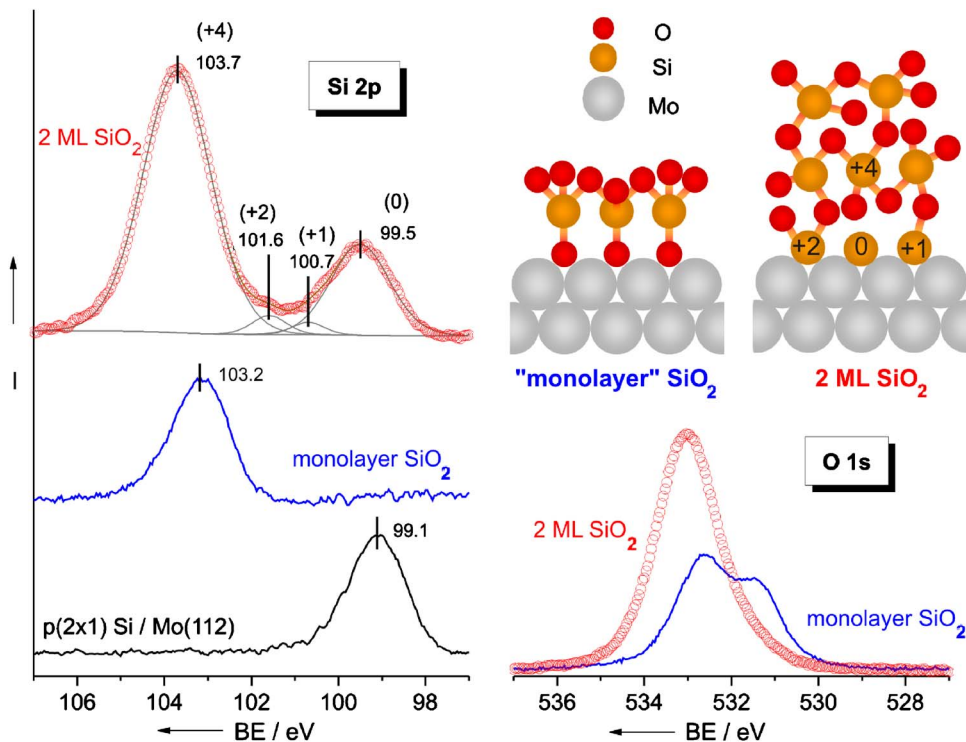


FIG. 1. (Color online) O 1s and Si 2p regions of XP spectra from monolayer and 2 MLE SiO<sub>2</sub> films on Mo(112). Si 2p region of an ordered surface MoSi<sub>x</sub> alloy is also shown. The top right shows a schematic model of monolayer and 2 MLE SiO<sub>2</sub> films.

a first-principles study of the growth of SiO<sub>2</sub> on MoSi<sub>2</sub>, where the most stable interface involved only Si<sup>+1</sup> and Si<sup>+2</sup> species.<sup>13</sup> The ratio of Si<sup>+1</sup>–Si<sup>+3</sup> to fully oxidized Si<sup>+4</sup> atoms is ~6% in our ~2 MLE films, substantially lower than the ~27% observed for ~2 MLE films grown on Si.<sup>2</sup>

LEED measurements of the multilayer films did not show diffraction spots, indicating a lack of crystallinity or long-range ordering. This is in agreement with studies on the passive oxidation of MoSi<sub>2</sub> alloys that show formation of amorphous SiO<sub>2</sub> films at 1500 K, and the appearance of crystalline phases only at temperatures >1700 K.<sup>14</sup>

IR spectra of amorphous multilayer SiO<sub>2</sub> films on Mo(112) and on Si (Refs. 2 and 15) substrates are shown in Fig. 2. The homogeneity of oxide films can be related to the full width at half maximum (FWHM) of their phonon peaks.

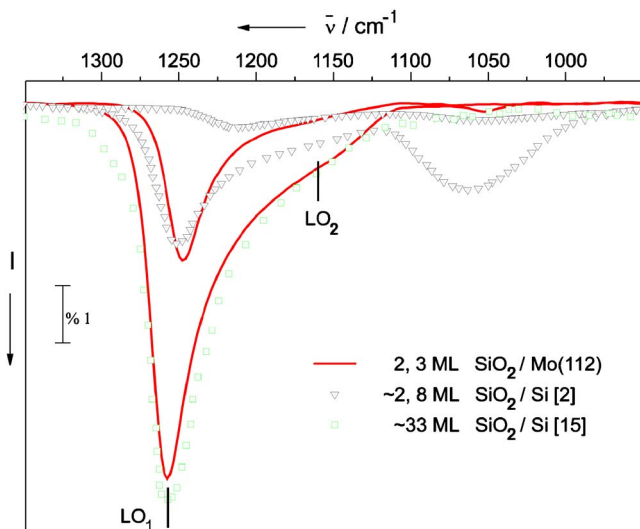


FIG. 2. (Color online) IR spectra of 2 and 3 MLE SiO<sub>2</sub> films grown on Mo(112). For comparison, the spectrum for amorphous SiO<sub>2</sub> films grown on Si (Refs. 2 and 15) substrates are shown with the reported optical modes LO<sub>1</sub> (1257 cm<sup>-1</sup>) and LO<sub>2</sub> (1160 cm<sup>-1</sup>) indicated.

The 3 MLE film presented here has a FWHM (for the ~1250 cm<sup>-1</sup> band) of ~50 cm<sup>-1</sup>, considerably better than the >100 cm<sup>-1</sup> obtained for similar films grown on Mo(112) by other methods.<sup>16</sup> When decreasing the thickness of the oxide films, the dominant trend in the IR spectra is a redshift in the asymmetric longitudinal optical (LO) phonon mode ~1250 cm<sup>-1</sup> (for SiO<sub>2</sub>/Si:  $\nu(\text{LO}_1)$ =1256, 1252, and 1219 cm<sup>-1</sup> for 100, 2.55, and 0.63 nm films, respectively<sup>2,15</sup>). The large shift (–37 cm<sup>-1</sup>) found for subnanometer SiO<sub>2</sub> films on Si has been attributed to the existence of a substoichiometric SiO<sub>x</sub> transition region.<sup>2</sup> A similar interpretation implies that the films on Mo(112) reach stoichiometry with 3 MLE (~0.9 nm, 1257 cm<sup>-1</sup>) and are only slightly perturbed at 2 MLE (~0.6 nm, 1248 cm<sup>-1</sup>).

A STM image of a film prepared using method 2 is shown in Fig. 3(a). The surface has an average roughness of ~0.1 nm on a 1 × 1 μm<sup>2</sup> scale. No monoatomic steps were resolved on multilayer films, although the steps of the substrate can be observed on the monolayer films [inset in Fig. 3(a)]. Figures 3(b) and 3(c) show STM images after deposition of Pd nanoparticles at 300 K. Early attempts to image particles on amorphous films produced low-resolution images.<sup>17</sup> However, the atomic smoothness of the films prepared in this work allows scanning of nanoparticles on amorphous films with similar quality to the results obtained on crystalline films.<sup>1</sup> In spite of the similarity (based on IRAS and XPS results) between films prepared by the three methods presented here, deposition of Pd nanoparticles on the films revealed differences on their surface morphology. Pd deposited on films grown by method 3 (using water/ice as oxidant) appears to decorate line defects [Fig. 3(c)]. This can be attributed to the formation of domain boundaries on the films prepared using water as an oxidant, reinforcing the prevailing notion that oxygen helps to prepare more homogeneous oxide films. In contrast to the reported diffusion of metal particles through monolayer films, no diffusion of Pd

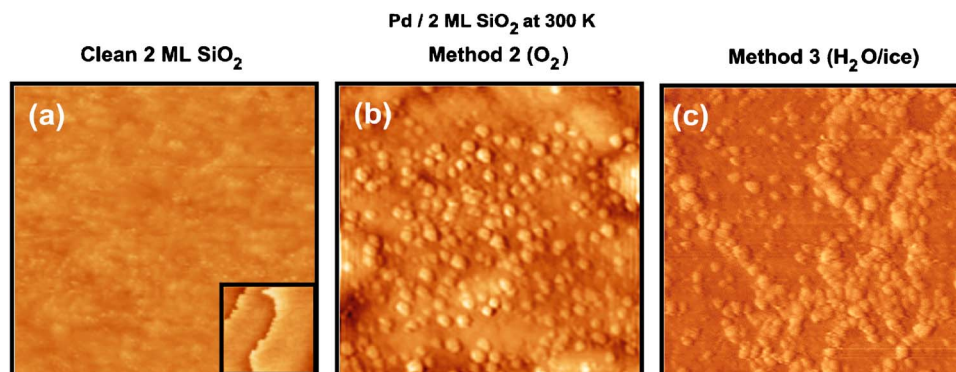


FIG. 3. (Color online) STM images of (a) a 2 MLE SiO<sub>2</sub> film grown on Mo(112) at 300 K using water as an oxidant (method 2). The inset shows an image of a monolayer SiO<sub>2</sub> film. [(b) and (c)] Images after deposition of Pd nanoparticles at 300 K on (b) a film prepared using oxygen as an oxidant (method 1) and (c) using water/ice as an oxidant (method 3). Size and tunneling parameters 100 × 100 nm<sup>2</sup>, V = 5.0 V, and I = 0.1 nA.

into the Si interface region of multilayer films was observed by XPS.

Even with the introduction of high- $\kappa$  dielectric oxides in MOS transistors, the presence of interfacial SiO<sub>2</sub>/Si is observed. Since metal silicides are already used as gates in transistors,<sup>18</sup> the results of this study suggest the possibility of producing sharper SiO<sub>2</sub> transition regions by the formation of silicide interfaces. Multilayer SiO<sub>2</sub> showing the properties of 100-nm-thick films can be grown with a thickness as small as  $\sim 0.6$  nm. The films do not show long range ordering but exhibit very smooth topography on a micrometer scale, which is ideal for their use as model oxides. The quality of thin oxide films can be improved using a two-step oxidation growth process, where the first step passivates the surface to prevent rapid oxygen diffusion into the interface and the second step fully oxidizes the film.

S.K. thanks the International Max Planck Research School (IMPRS) “Complex Surfaces in Materials Science,” and J.W. and D.S. the Alexander von Humboldt Foundation for fellowships. We would like to thank Gianfranco Pacchioni for fruitful discussions. The work was supported by the EU Project GSOMEN.

<sup>1</sup>H. Freund, Surf. Sci. **500**, 271 (2002).

<sup>2</sup>K. T. Queeney, M. K. Weldon, J. P. Chang, Y. J. Chabal, A. B. Gurevich, J. Sapieta, and R. L. Opila, J. Appl. Phys. **87**, 1322 (2000).

<sup>3</sup>J. W. He, X. Xu, J. S. Corneille, and D. W. Goodman, Surf. Sci. **279**, 119 (1992).

<sup>4</sup>T. Schroeder, M. Adelt, B. Richter, M. Naschitzki, J. B. Giorgi, M. Bäumer, and H.-J. Freund, Surf. Rev. Lett. **7**, 7 (2000).

<sup>5</sup>H. J. Freund, Surf. Sci. **601**, 1438 (2007).

<sup>6</sup>L. Giordano, A. Del Vitto, and G. Pacchioni, J. Chem. Phys. **124**, 034701 (2006).

<sup>7</sup>S. Kaya, Y. N. Sun, J. Weissenrieder, D. Stacchiola, S. Shaikhutdinov, and H.-J. Freund, J. Phys. Chem. C **111**, 5337 (2007).

<sup>8</sup>J. Pantfölder, R. Dornick, Ch. Ammon, G. Held, and H. P. Steinrück, Surf. Sci. **480**, 73 (2001).

<sup>9</sup>K. T. Queeney, M. K. Weldon, Y. J. Chabal, and K. Raghavachari, J. Chem. Phys. **119**, 2307 (2003).

<sup>10</sup>J. Weissenrieder, S. Kaya, J.-L. Lu, H.-J. Gao, S. Shaikhutdinov, H.-J. Freund, M. M. Sierka, T. K. Todorova, and J. Sauer, Phys. Rev. Lett. **95**, 076103 (2005).

<sup>11</sup>S. Kaya, M. Baron, D. Stacchiola, J. Weissenrieder, S. Shaikhutdinov, T. K. Todorova, M. Sierka, J. Sauer, and H.-J. Freund, Surf. Sci. **601**, 4849 (2007).

<sup>12</sup>N. Ohishi, H. Yanagisawa, K. Sasaki, and Y. Abe, Electron. Commun. Jpn., Part 2: Electron. **84**, 71 (2001).

<sup>13</sup>D. E. Jiang and E. A. Carter, Phys. Rev. B **72**, 165410 (2005).

<sup>14</sup>G. Reisel, B. Wielage, S. Steinhauser, I. Morgenthal, and R. Scholl, Surf. Coat. Technol. **146**, 19 (2001).

<sup>15</sup>C. T. Kirk, Phys. Rev. B **38**, 1255 (1988).

<sup>16</sup>S. Wendt, E. Ozensoy, T. Wei, M. Frerichs, Y. Cai, M. S. Chen, and D. W. Goodman, Phys. Rev. B **72**, 115409 (2005).

<sup>17</sup>X. Xu, J. Szanyi, Q. Xu, and D. W. Goodman, Catal. Today **21**, 57 (1994).

<sup>18</sup>E. P. Gusev, V. Narayanan, and M. M. Frank, IBM J. Res. Dev. **50**, 387 (2006).